UvA-DARE (Digital Academic Repository)

Fluid Simulations with Atomistic Resolution: Multiscale Model with Account of Nonlocal Momentum Transfer

Svitenkov, A.I.; Chivilikhin, S.A.; Hoekstra, A.G.; Boukhanovsky, A.V.

Link to publication

Citation for published version (APA):
Svitenkov, A. I., Chivilikhin, S. A., Hoekstra, A. G., & Boukhanovsky, A. V. (2015). Fluid Simulations with Atomistic Resolution: Multiscale Model with Account of Nonlocal Momentum Transfer. *Procedia Computer Science*, *51*, 1108-1117. https://doi.org/10.1016/j.procs.2015.05.279

Fluid simulations with atomistic resolution: multiscale model with account of nonlocal momentum transfer

Andrew I. Svitenkov[1], Sergey A. Chivilikhin1, Alfons G. Hoekstra[1,2] and
Alexander V. Boukhanovsky[1]

[1]*ITMO University, Saint Petersburg, Russia*
[2] *University of Amsterdam, The Netherlands*
svitenkov@yandex.ru.com, sergey.chivilikhin@gmail.com,
a.g.hoekstra@uva.nl, avb_mail@mail.ru

Abstract

Nano- and microscale flow phenomena turn out to be highly non-trivial for simulation and require the use of heterogeneous modeling approaches. While the continuum Navier-Stokes equations and related boundary conditions quickly break down at those scales, various direct simulation methods and hybrid models have been applied, such as Molecular Dynamics and Dissipative Particle Dynamics. Nonetheless, a continuum model for nanoscale flow is still an unsolved problem. We present a model taking into account nonlocal momentum transfer. Instead of a bulk viscosity an improved system of parameters of liquid properties, represented by a spatial scalar function for momentum transfer rate between neighboring volumes, is used. Our model does not require boundary conditions on the channel walls. Common nanoflow models relying on a bulk viscosity in combination with a slip boundary condition can be obtained from the model. The required model parameters can be calculated from momentum density fluctuations obtained by Molecular Dynamics simulations. Thus, our model is multiscale, however, the continuum model is applied in the whole region of the simulation. We demonstrate good agreed with nanoflow in a tube as obtained by complete Molecular Dynamics.

Keywords: Multiscale simulation, fluid dynamics, transfer processes, Green–Kubo relations, molecular dynamics, nanoscale flow

1 Introduction

Methods such as Molecular Dynamics (MD), Dissipative Particle Dynamics (DPD), and Direct simulation of Monte Carlo (DSMC) have played an important role in the field of nanomechanics. Their most considerable advantage is their applicability for study of materials and systems where the relation between macroscopic properties and atomistic processes is difficult to understand. The present paper specifically focuses on micro- and nano-scale fluid dynamics, which is a classic case of such

systems. Navier-Stokes Equation (NSE) with Green-Kubo relations for viscosity provide an example of a model of relations for atomistic processes and macroscopic mechanical properties of the bulk liquid. Unfortunately, in a nanoflow, the continuum NSE and related boundary conditions break down, as was demonstrated in experimental studies (Li, et al., 2007) and by MD simulation (Joseph, et al., 2008). MD reproduces fluid behavior at atomistic scales and so is the most accurate model of any mechanical properties of a liquid. Since in principal a flow problem could be entirely described by MD, it is commonly used for validation of approximate models of nanoflows with examples of small systems and simulating over short time-scales, such as water permeation through a carbon nanotube. At the same time applied nano- and micro-engineering problems become computationally intractable for MD. To develop methods that resolve the nanoscale flow phenomena accurately and efficiently some attempts to modify NSE and related boundary conditions were undertaken (Hansen, et al., 2011), (Reese, et al., 2007). The most well-known method is the introduction of a slip boundary condition with corresponding coefficient of slip length. A priori estimation of the slip length is the main complication of this approach (To, et al., 2013). Generally a dependence of slip length on the Knudsen number is assumed (Shokouhmand., et al., 2010), (Reese, et al., 2007). Other semi-empirical parameters such as the tangential momentum accommodation coefficient were considered (Prabha, et al., 2012). However, all Knudsen-based approaches are physical well resolved only for the case of a gas flow. For a liquid the slip length and corresponding quantities are usually applied only for comparative description of flows or as empirical parameters estimated by experimental or MD simulation studies.

More radical attempts to construct continuum nanoflow model were also undertaken. They include modifications of NSE with by account of rotational degrees of freedom of molecules (Hansen, et al., 2011), quantum effects (Popov, 2011) and even structural features of water (Chivilikhin, et al., 2008). However, we are not aware of real applications of these methods.

We observe a decline of interest in continuum nanoflow models in favor of multiscale simulation methods, containing coupled atomistic (MD) and continuum models (Asproulis, et al., 2012). We however present a novel continuum nanoscale model of a liquid with a multiscale bridging method. The structure of our multiscale approach is noticeable different from the usual atomistic-continuum coupling. We will introduce our model, discuss the main distinctions with standard methods, and discuss where and how our model could be more effective.

The most common approach to hybrid methods for dense fluids is domain-decomposition (DD). As the name implies, the computational domain is divided into macro and micro parts with some overlap. Micro parts are usually a boundary region or other heterogeneous regions in the fluid. They are considered small relative to bulk domains. Such combination saves computational resources in comparison with full MD models and the question about a correct continuum nanoscale model is less complicated. Because of this the emphasis of multiscale nanoflow simulation studies is on a detailed consideration of multiscale bridging algorithms (Fedosov, et al., 2009). Unfortunately, DD still contains a considerable computational inefficiency. For the simplest continuum model, such as the usually applied NSE, the size of the microscopic domains is too big and the computational efforts for the MD part quickly become quite expensive. This may seem like a reasonable trade-off between accuracy of a full continuum model and computational cost of a hybrid model. Yet some models containing more complex (so-called mesoscopic) models, like Dissipative Particle Dynamics (DPD) and Lattice-Boltzman Methods (LBM), were developed (Fedosov, et al., 2009), (Dupuis, et al., 2007). However, the systems of parameters for both models were chosen as for a viscous liquid. The values of the parameters were not calculated with a multiscale simulation. They were in fact chosen as constants corresponding to a viscosity of the studied liquid. To conclude, we do not see why the mesoscopic solutions should be considerable different relative to NSE solutions.

More flexible multiscale techniques are the Heterogeneous Multiscale Method (HMM). In this type of multiscaling the domain is entirely described by the macro model, with small isolated micro models spatially distributed in the domain (E, et al., 2007). Like DD methods, micro resolution is

required in regions close to bounding surfaces and constrained from the continuum strain-rate field, and in turn provide an accurate local velocity slip and stress at the wall. In other words microscale regions provide information about liquid properties through the system of prameters, which are present in the governing equations of the continuum model and indirectly influence the solution. This may be for instance an additional non-viscous tensor of shear stresses and a slip rate as in (Borg, et al., 2013) or a pressure correction in (Borg, et al., 2013). One way or another, HMM in nanoflows supposes a modification of the continuum NSE model. So, the quality of the final hybrid model depends on such modification, which, however, usually is proposed by in phenomenological way without fundmental explanation. It should be noted, that the issue of NSE correction and multiscale bridging is related since for the new set of parameters the corresponding calculation method has to be proposed too. While for classical viscous or elastic models of media ways to compute parameters (such as viscosity, Young's modulus, and so on) are known, this may be less clear for applications of new and more complex models (Hansen, et al., 2011). We have seen that some powerful simulation methods such as DPD and LBM cannot be easily used in a multiscale approach due to this reason. For example, an interacted process of momentum transfer can be described by LBM, that is demonstrated in (Lorenz, et al., 2011). The proposed multiscale model gives a good approximation of non-Newtonian behavior of suspension due to account of dependences of viscosity on volume fraction and share-rate (i.e. nonlinear behavior) however, the standard viscous collision operator was used, which describes only local, isotropic and instant response. We will show below that such artificial restriction may lead to considerable inaccuracy, which is unavoidable by account of nonlinearity or by space-dependent viscosity. Even in the case of simulation of nanoscale liquid properties, where deviations from the momentum transfer from classical approaches is considerable, the standard viscous collision term is used too (Mackay, et al., 2013). We are not aware of studies where more complex parameterization of the collision term were used.

The purpose of this study is construction of a hybrid nanoscale liquid model "from bottom to top". To do so, a continuum model of momentum transport has to be derived systematically from microscopic relations that simultaneously gives estimations for the limits of applicability of our continuum model and clear calculation method for the system of parameters of it.

Note, that in the field of multiscale nanocomposite simulation similar HMM approaches are used and close problems with ways of calculating continuum model parameters exist (Yang, et al., 2013). Therefore, we believe that our multiscale coupling method may be useful in a more general sense.

2 Continuum model of nanoflow

Many researchers believe NSE is exact, but it contains some hidden assumptions, which are incompatible with conditions of nanoflow.

2.1 Broken NSE and a condition of translational invariance

Consider a scalar conserved quantity $a=a(\mathbf{r})$, such as a concentration. Vector $\mathbf{r}$ is a real-space position in the region of interest. We also introduce the flux of a, denoted by $\mathbf{j}_a=\mathbf{j}_a(\mathbf{r})$. They are related by the exact microscopic equation:

$$\frac{\mathrm{d}\hat{a}(\mathbf{r})}{\mathrm{d}t} = -\nabla\hat{\mathbf{j}}(\mathbf{r}),\qquad(2.1)$$

where the hat denotes microscopic values (i.e. obtained by MD simulation, for example). We also can write something for average of $\mathbf{j}_a$ and a. As diffusive transport is driven by the gradient of a quantity, the expression

$$\mathbf{j} = -\eta\nabla a \qquad (2.2)$$

is often used. With (2.1) it gives a common diffusion equation with η as diffusion coefficient. In particular, it describes the viscous momentum transfer in NSE for an uncompressible liquid. However, (2.2) isn't exact and the general case may be more complex:

$$\mathbf{j}(\mathbf{r}, t) = \int_0^\infty \int_V G(\mathbf{r}, \mathbf{r}', \tau) \nabla a(\mathbf{r}', t - \tau) d\mathbf{r}' \, d\tau \qquad (2.3)$$

The core function G is characterized by a correlation length r_c and memory time τ_c,– the distance $|r - r'|$ and delay t-τ where G vanishes. We will consider zero memory time assumption in the following that eliminates the time integration. The simplest way to deal with the space integration is to assume $r_c \to 0$, or ∇a changes little in this neighborhood. We can expect that in the case of nanoflows this approach is incorrect. Eq. (2.2) however remains a good approximation if the space symmetry of G holds true, so if $G(\mathbf{r}, \mathbf{r}') = G(\mathbf{r}', \mathbf{r})$. Indeed, in this case (2.3) and (2.1) results in (in zero memory time assumption):

$$S(\mathbf{r}) = -\nabla \int_V G(\mathbf{r}, \mathbf{r}') \nabla a(\mathbf{r}') d\mathbf{r}' = \int_V G(\mathbf{r}, \mathbf{r}') \Delta a(\mathbf{r}') d\mathbf{r}' \approx \eta^{-1} \int_V G(\mathbf{r}, \mathbf{r}') S(\mathbf{r}') d\mathbf{r}' \qquad (2.4)$$

where source: $S(\mathbf{r}') = \dot{a}(\mathbf{r}')$. We have used a space-locality approach for the last equality, and we wonder how accurate this equality is? If G is translation invariant the last equality in (2.4) has a second order of accuracy on r_c because:

$$S(\mathbf{r}) \approx \eta^{-1} \int_V G(\mathbf{r} - \mathbf{r}')(S(\mathbf{r}) + S'(\mathbf{r})(\mathbf{r}' - \mathbf{r}) + o(|\mathbf{r}' - \mathbf{r}|^2) d\mathbf{r}' \quad (2.5)$$

is a second-order approximation if the translation invariant G is even. In this case the integral with an odd first-order term gives zero. So, in the case of translational invariance of the core function G the last equality in (2.4) has a second order of accuracy on r_c. Therefore, the impact of geometry as expressed in G is more relevant compared to variations of $a(\mathbf{r})$. This is not surprising, but interesting because this feature is implicitly used in domain decomposition multiscale approaches. We can see why the structure of the microscopic and macroscopic domains in hybrid models depends only on geometry of the channel and we do not have to adjust them dynamically with the evolution of the solution $a(\mathbf{r})$. The consequences for boundary conditions are also implied as will be shown in detail below.

2.2 Continuum nanoscale model for a fluid

According to the theory of linear response to a disturbance δF, the time of evolution of the quantity of interest $A(\mathbf{r}, t)$ is given by:

$$A(\mathbf{r}, t) = \left\langle \hat{A} \right\rangle_0 + \frac{1}{kT} \int_0^\infty \int_V \left\langle \hat{A}(\mathbf{r}, t) \dot{\hat{B}}(\mathbf{r}', t - \tau) \right\rangle F(\mathbf{r}', t - \tau) d\tau d\mathbf{r}', \qquad (2.6)$$

where $\left\langle \hat{A} \right\rangle_0$ gives undisturbed value of A, B is defined by $\delta \hat{h}(r, t) = \hat{B}(r, t) \delta F(r, t)$. Here h is an energy density at point $\mathbf{r}$ and time t. The correlation term is the so called response function $\varphi_{A\dot{B}}$ (the dot above B denote time derivative just as in (2.3)). The hat above a symbol denotes its microscopic analogue. For the general viscoplastic problem momentum flow $j_{\alpha\beta} = v_\beta p_\alpha + \delta_{\alpha\beta} P + \sigma_{\alpha\beta}$ ($\sigma_{\alpha\beta}$ is a stress tensor, P is the pressure, and p_α, v_α are the α-component of momentum and velocity respectively). Greek indices enumerate Cartesian coordinates $\{x, y, z\}$. The disturbance of the full energy density due to third term is $\delta h = \partial \sigma_{\alpha\beta} / \partial x_\beta \cdot \delta u_\alpha$ (summation over dummy indices is assumed). So, from (2.6) follows:

$$\sigma_{\alpha\beta}(\mathbf{r}, t) = \frac{1}{kT} \int_V \int_0^\infty \left\langle \sigma_{\alpha\beta}(\mathbf{r}, t) \frac{\partial}{\partial x_\gamma} \dot{\sigma}_{\lambda\gamma}(\mathbf{r}', t - \tau) \right\rangle u_\lambda(\mathbf{r}', t - \tau) d\tau d\mathbf{r}' \qquad (2.7)$$

Note that the response function (the correlation term) is considered as function of τ only (not of t) since property of medium usually is constant or slow variable. By space integration by parts, we can carry out the space derivative from the response function, wherein the nonitegral term becomes zero. Next, by temporal integration by parts we obtain:

$$\sigma_{\alpha\beta}(\mathbf{r},t) = -\int_V K_{\alpha\beta\lambda\gamma}(\mathbf{r},\mathbf{r'})\frac{\partial}{\partial r'_\gamma}u_\lambda(\mathbf{r'})d\mathbf{r'} - \int_0^\infty\int_V G_{\alpha\beta\lambda\gamma}(\mathbf{r},\mathbf{r'},\tau)\frac{\partial}{\partial r'_\gamma}v_\lambda(\mathbf{r'},t-\tau)d\tau d\mathbf{r'} \quad (2.8)$$

where by $K_{\alpha\beta\lambda\gamma}$ and $G_{\alpha\beta\lambda\gamma}$ we have denoted the instantaneous part of the response function, which corresponds to elastic response, and the non-instantaneous part corresponding to viscous response. We will not consider elastic response in this paper, because of the hydrodynamic assumption (weak and slow impact). The second term is equivalent to (2.3).

The thermodynamic theory of linear response contains some assumption, which should be noted. The first is a quasi-equilibrium state of the disturbed system. This means that the state of the system is still fully determined by average values of quantities of interest (the full set being density, energy density, momentum density). This is the main limitation of our model, but we are not aware of any reports on such flow regimes. Another obvious limitation is the linear response of the molecular system. An additional assumption, is isotropy of the response ($G_{\alpha\beta\lambda\gamma} = G\delta_{\alpha\lambda}\delta_{\beta\gamma}$). It is valid only far from boundaries and for strongly confined fluids consideration of the response tensor $G_{\alpha\beta}$ is preferred (Hartkamp, 2012). The final governing equation for the momentum density is Eq. (2.9), which results from the combination of the continuity condition (2.1) and (2.8):

$$\frac{\partial p_\alpha}{\partial t} + v_\beta\frac{\partial p_\alpha}{\partial r_\beta} = -\frac{\partial P}{\partial r_\alpha} + \frac{\partial}{\partial r_\beta}\int_0^\infty\int_V G_{\alpha\beta}(\mathbf{r},\mathbf{r'},\tau)\frac{\partial v_\alpha(\mathbf{r'},\tau)}{\partial r'_\beta}d\tau d\mathbf{r'}, \quad (2.9)$$

where all values implicitly correspond to time t and space point $\mathbf{r}$. Note that (2.9) turns into NSE with the assumption of temporal and space locality (and transitional invariance) of the response function. The resulting expression for the viscosity will be equal to the well-known Green-Kubo expression. More interesting, however, is an intermediate approach, leading to the slip boundary condition, which is relevant for the description of flow in nanochannel (Joseph, et al., 2008). As this transition is not immediately obvious the next sections quickly reviews this step.

2.3 Boundary conditions

Our continuum model of fluid flow does not require any special conditions at the wall of the channel. The only requirement is a zero mass velocity $\mathbf{v}$ at infinity. Indeed, expression (2.9) is suitable for description of viscous momentum transfer both in the liquid and in the solid walls. No "boundaries" of the channel exist as they are implicitly expressed by $G_{\alpha\beta}(\mathbf{r},\mathbf{r'},\tau)$, and so no "boundary condition" is required. The necessity of a wall boundary conditions (BC) is the consequence of the assumption of translational invariance of rheological response in the bulk, which of course is broken near the wall.

In our simulation we will assume zero velocity of the channel walls and describe momentum transfer with the full expression (2.9), but only in the inside region of the channel. However, in some cases a near wall model formulated as a BC may be useful. For the classical case the standard zero velocity BC means that all momentum received by the boundary layer of liquid is immediately scattered at the wall. For nanochannels however, the interaction between liquid and wall is considered weak, leading to the well-known slip BC:

$$v_t\big|_{z=0} = l\left(\frac{\partial v_t}{\partial z}\right)\bigg|_{z=0} \quad (2.10)$$

where v_t is a tangential component of velocity, and the wall is at the $z=0$ plane. To derive (2.10) from (2.9) we assume velocity depends on the z-coordinate only and $G(\mathbf{r},\mathbf{r'},\tau) = G(z,\mathbf{r'},\tau)$ too. Here only

tangential component of momentum and its transfer only in normal direction are considered, therefore scalar response G instead $G_{\alpha\beta}$ is used.

By integration over the plane (x,y) we obtain:

$$f_x + \frac{dP}{dr_x} = \frac{\partial}{\partial r_z} \int_{-\infty}^{\infty} S(z,z') \frac{\partial v_x(z')}{\partial z'}_z dz', \qquad (2.11)$$

where we also assume $\mathbf{v}=\{v_x,0,0\}$; $\mathbf{f}$ is a specific force acting upon a wall-liquid surface junction (Pa/m); This situation is depicted in Figure 1 as the "exact" case. For the "approximation" case the region of dependence of S on z is considered thin and located at $z=0$. Wherein the dependence on z' comes discontinuous: $S(z')=S_w(z') (1-\Theta(z'))+ S_l(z') \Theta(z')$ ($\Theta(z')$ is the unit step function). Then by integration by part we carry out the space derivative in Eq. (2.11) and obtain a Dirac delta function from $S(z')$ (singularity at $z'=0$). Additionally we assume that the gradient pressure force is small in comparison with tensions produced by the $G(\mathbf{r},\mathbf{r'})$ gap. The final relation is:

$$f_x = l \frac{\partial v_x}{\partial z} \sim v_x, \qquad (2.12)$$

where l is some constant related to the size of the gap of $S(z')$ at $z'=0$. Expression (2.10) is written relative to velocity and we can propose only a phenomenological proportionality for tangential surface tension and slip velocity (the last relation). Therefore our model (2.9) implies both the slip boundary condition and classical NSE approach and thus includes another less acurate model of liquid flow.
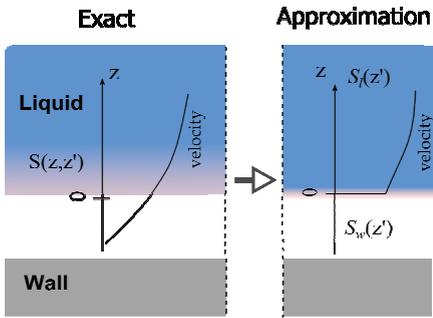
Figure 1 Slip approximation for boundary region. Blue area corresponds to liquid, white to the channel wall. Consideration of δ layer as thin leads to slip phenomenon
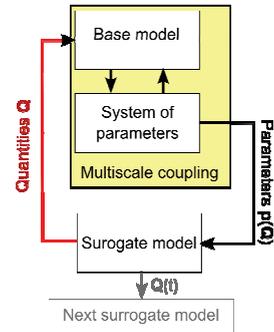
Figure 2 Schematic diagram of suggested multiscale approach structure

3 Multiscale bridging

The multiscale bridging method consists of a computational procedure to obtain parameters of our continuum model, relying on atomistic MD simulations of a liquid. The core function $G_{\alpha\beta}(\mathbf{r},\mathbf{r'})$ determines momentum transport properties of media, see Eq. (2.9). Therefore it forms the required parameter system. It can be represented as a finite set of numbers by discretization upon a space mesh.

Our approach of multiscale bridging is inspired by (Oden, et al., 2006). A two-level multiscale model combines *surrogate* and *base* models. The first is given by (2.9) and is an approximate model and the second is a finest microscopic model of a real system represented by MD simulation. Let $\mathbf{Q}$ denote a vector of quantities of interest, which could be calculated with either the base model by some averaging or by the surrogate model. We would like to minimize the difference between Q computed with the surrogate and base model: $\left\| \mathbf{Q}(t) - \hat{\mathbf{Q}}(\mathbf{u}(t)) \right\| \to \min$, where $\mathbf{u}(t)$ is a full phase space vector of the state of the molecular system. Let L be the *surrogate evolution operator* such that $\partial \mathbf{Q}/\partial t = \mathrm{L}\,\mathbf{Q}$. We call the appearance of L and corresponding set of parameters the *parameterization* of a base

system or the system of parameters of the surrogate model. Our full surrogate model is described by Eq. (2.9). We will however use the expression:

$$\mathbf{j}_\alpha(\mathbf{r},t) = -\int_0^\infty \int_V \mathbf{G}_\alpha(\mathbf{r},\mathbf{r}',\tau)\nabla v_\alpha(\mathbf{r}',t-\tau)d\mathbf{r}'d\tau + P\mathbf{e}_\alpha + \mathbf{v}p_\alpha \qquad (3.1)$$

which is more convenient for multiscale bridging, because it contains only one spatial derivative. So, the formulation of $\hat{L}$ is given by expression (2.9), $G_{\alpha\beta}(\mathbf{r},\mathbf{r}')$ is a parameterisation and $\mathbf{Q}$ represents the momentum density flux tensor for each point of the simulation region.

A schematic diagram of the multiscale computational algorithm is shown in Figure 2. The black arrow denotes the fact that the parameter values are calculated for the dynamics of the quantities of interest. Our multiscale bridging procedure consists of using fluctuation dynamics of momentum density and mass velocity obtained by MD simulations as a source for the optimization problem.

At the "base model" stage all values of $\mathbf{p}$, $\mathbf{v}$, $\mathbf{j}_\alpha$ in (3.1) is calculated for discretisation volumes. For momentum flow we have used the following microscopic expression:

$$j_{\alpha\beta} = \frac{1}{n}\sum_i \frac{p_{i\alpha}p_{i\beta}}{m} - \frac{1}{2n}\sum_i \frac{r_{ij\alpha}r_{ij\beta}}{r_{ij}} f_{ij}, \qquad (3.2)$$

where i enumerates all n atoms belonging to a given discretization volume; j does not belong to given discretization volume; r_{ij} – is the length of $\mathbf{r}_{ij} = \mathbf{r}_j - \mathbf{r}_i$, f_{ij} the length of the force vector. (The expression is intended for a simple fluid MD model.) The pressure term in (3.1) is assumed to be zero.

Substitution of the time series of microscopic dynamics in a discrete form of (3.1) results in a system of linear equations (SLE):

$$j_i^t = \sum_{j,\tau} g_j^{t,\tau}G_{ij}^\tau \qquad (3.3)$$

where $\nabla v_\alpha(\mathbf{r}',t-\tau)$ is denoted by $g_j^{t,\tau}$ and Greek indices are omitted for brevity, $G_{\cdot j}^\tau$ is desired vector. The Greek indices for tensor $G_{\alpha\beta}$ are omitted too and that each component should be considered separately is implied. Subscript indices enumerate vertices of a space mesh and the superscript index enumerates time intervals. I.e. each row of $\mathbf{G}$ (i-indexed) is calculated independently.

The number of equations depends on the length of the time series (number of measurements of α-component momentum flow). Note, that the solution of such overdetermined system of equations by a least-squares method is a solution of a minimization of the difference between $\hat{\mathbf{j}}_\alpha(\mathbf{r})$ observed with MD simulation and those from the surrogate model.

Consider matrix $\mathbf{g}$ of system (3.3). Its columns are history of momentum density at the space point r_j with time t-τ. The method of least squares leads to the matrix of scalar products of $(\mathbf{g}_j^0,\mathbf{g}_k^\tau)$. Due to locality of momentum fluctuations we have to measure the momentum density with small time step for a diagonally dominant matrix. Otherwise, for the time intervals τ larger than the correlation time τ_c diagonal elements like $(\mathbf{g}_j^0,\mathbf{g}_j^\tau)$ will not be close to 0, as well as non-diagonal. Hence the reason why we cannot carry out the time integration in (2.9) beforehand is, despite the stationary character of the flow problem.

4 Results and discussion

As a case study we will consider elementary problem of liquid flow in a nanotube (Borg, et al., 2013), Figure 3. The dependence of velocity on radial coordinate r is considered. Using the symmetry of the problem we can simplify (2.9), and after time integration we get:

$$\frac{dP}{dz} = const = \nabla_{xy}\int_S K(\mathbf{s},\mathbf{s}')\nabla_{xy}p_z(\mathbf{s}')d\mathbf{s}', \qquad (4.1)$$

where S is a cross section of the tube.

The calculation of K were based on MD simulation. We have used a model of a simple fluid like

Andrew I. Svitenkov, Sergey A. Chivilikhin, Alfons G. Hoekstra and Alexander V. Boukhanovsky

liquid argon at 86K, equilibrium pressure 1 bar. A 10 nm diameter carbon nanotube with a length of 30 nm was chosen as a channel. We used the Lennard-Jones (LJ) potential in Amber form with length parameters 3.734Å for Ar and 3.985Å for C, energy -0.238kcal/mol for Ar and -0.07kcal/mol for C. Carbon atoms were fixed. The measurements of density, momentum density and momentum density flow were performed (for the last Eq. (3.2) was used) with averaging over the cell, depicted in figure 4, (square, step 3.734Å). The space derivative was calculated with a symmetry pattern. Then the time-dependent volume core function was found by SLE (3.3) (time-dependent), and by integration in time and along the z-coordinate the plane core function K was obtained. Note that only one component of $G_{\alpha\beta}$, which describe the transfer of z-momentum in radial direction is considerable due to symmetry and therefore the K function is a scalar. All measurements were performed at the central 10nm tube fragment.
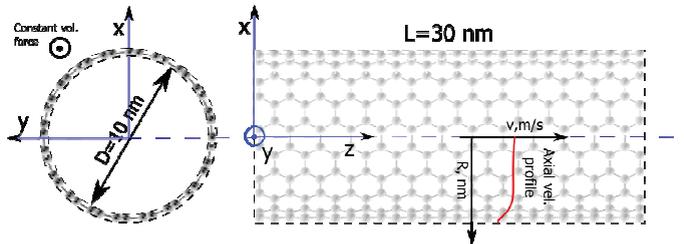
Figure 3 Poiseuille problem formulation: D is the tube (nanotube) diameter, L the tube length

Because the discretization step was chosen equal to Ar-Ar LJ interaction length, the core function occupies ~10 discretization elements only. This is shown in the right picture in Figure 4 by a color map of $K(\mathbf{s},\mathbf{s}')$ for a near-wall position $\mathbf{s}$. The time step was equal to 1fs and τ_{corr} was taken 2ps.
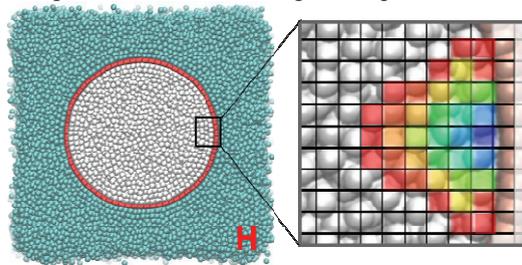
Figure 4 Cross section of the MD simulation and averaging cells with colour map of core function K (blue is high, red is low).

In Figure 5 $K(\mathbf{s},\mathbf{s}')$ is shown for some different space points. The asymmetry of the core function is minimal for R=2nm (R=|$\mathbf{s}$|) and maximum for the near-wall region (R=4.5nm). This means weak correlations between atoms of the nanotube and atoms of the liquid (because of much stronger bonds between the first) and leads to a near-wall slip. The central region of the tube where the core function asymmetry is weak was marked as a NSE-region. We have obtained fluctuations at two conditions: equilibrium (without flow) and nonequilibrium, driven by a gravity-like constant force f=0.1 cal/mol/Å flow. In Figure 5 the nonequilibrium system of parameters $K(\mathbf{s},\mathbf{s}')$ for some different space points are depicted too (lower half).

After calculation of the system parameters for both the equilibrium and non-equilibrium cases, equation (4.1) was solved. It was considered as SLE by discretization at the same mesh that was used for averaging of MD data.

The solutions, which have been found for the equilibrium and nonequilibrium cases are shown in Figure 6. There are two axial velocity profiles. The third velocity profile were obtained by direct MD simulation of the flow (the same gravity-like constant force f=0.1cal/mol/Å was applied) and is the reference solution. The surrogate velocity profile obtained with the nonequilibrium set of parameters

(blue solid line) is very close to the result of the MD simulation.

All MD simulations were performed with the NAMD molecular dynamics package. During observation of momentum density fluctuations no thermostat algorithms were used.
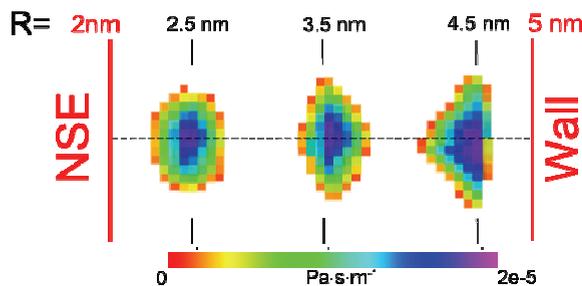
Figure 5 Colormaps for the core function *K* for the different radii, **s'**=0 corresponds to the center of each core function, plane of picture is a XY plane, dashed line is a diameter, the top-half and bottom-half are for the equilibrium and flow conditions respectively
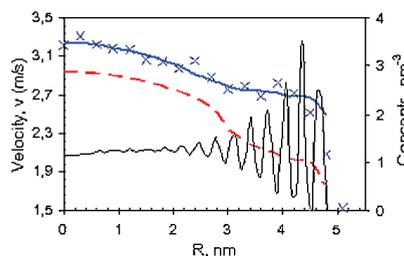
Figure 6 Velocity and density axial profiles: blue crosses is the results of direct MD simulation, red dashed line is a velocity profile for *K* measured in equilibrium, solid blue line is a velocity profile for *K* measured during the flow, and the black line is the density.

5 Conclusion

We propose a multiscale model of nanoscale fluid flow. The main feature of our approach consists of a systematic derivation of the continuum surrogate model that leads to noticeable changes in the whole structure of the hybrid model.

A continuum model of liquid was considered without assuming a local character of momentum transfer. An important result is the disappearance of unnatural boundary condition for the velocity. The slip boundary condition may be obtained as some intermediate assumption of (2.9).

The main point in our approach is the method of multiscale bridging, i.e. the method of computing the complex system of parameters. As the calculation of the core integral function from (2.9) by direct averaging may turn out to be difficult, a method based on direct comparison of dynamics of quantities of interest obtained by MD and the surrogate simulation was proposed. The one important feature of this multiscale coupling method is a completely different character of the microscopic and macroscopic dynamics of the momentum density. It is a "boiling pot" of fluctuations for the first and a diffusion process for the last, which is the result of averaging over many trajectories. Nonetheless, we did not have to introduce any additional averaging procedures. All averaging assumed by the surrogate model is implemented implicitly.

However, the results of the multiscale simulation turned out not as good as we expected. Despite our theoretical analysis from subsections 2.1 and 2.2 there is a feedback influence of resulting velocity profile on the values of parameters of the surrogate model. We surmise this is result of influence of nonzero average velocity to thermodynamic state of liquid. Since parameter values were calculated for the equilibrium state of the liquid inaccuracy occurred, thus for a better result the fluctuation dynamics, which determines momentum transfer processes, should be obtained in condition of flow. However, an important issue arises here: how one represents nonequilibrium macroscopic conditions at the atomistic base model (red arrow at the Figure 2). This problem is outside the scope of this study, but it was already analyzed in detail in many studies about hybrid multiscale nanoflow models.

Acknowledgments

References

Asproulis, N., Kalweit, M., & Drikakis, D. (2012). A hybrid molecular continuum method using point wise coupling. *Advances in Engineering Software Volume 46, Issue 1* , 85–92.

Borg, M. K., Lockerby, D. A., & Reese, J. M. (2013). A multiscale method for micro/nano flows of high aspect ratio. *J. of Computational Physics 233* , 400-413.

Borg, M. K., Lockerby, D. A., & Reese, J. M. (2013). Hybrid continuum-molecular modelling of multiscale internal gas flows. *J. of Computational Physics 255* , 149-165.

Chivilikhin, S. A., Gusarov, V. V., Popov, I. Y., & Svitenkov, A. I. (2008). Model of fluid in nanochannel. *Russian J. of Math. Phys. 15 No 3* , 409–411.

Dupuis, A., Kotsalis, E. M., & Koumoutsakos, P. (2007). Coupling Lattice Boltzmann and molecular dynamics models for dense fluids. *Phys. Rev. E 75 046704* .

E, W., Engquist, B., Li, X., Ren, W., & Vanden-Eijnden, E. (2007). Heterogeneous Multiscale Methods: A Review. *Commun. Comput. Phys., Vol. 2* , 367-450.

Fedosov, D. A., & and Karniadakis, G. E. (2009). Triple-decker: Interfacing atomistic-mesoscopic-continuum flow regimes. *J. Computational Physics* , 1157-1171.

Hansen, J. S., Dyre, J. C., Daivis, P. J., Todd, B. D., & Bruus, H. (2011). Nanoflow hydrodynamics. *Phys. Rev. E 84, 036311* .

Hansen, J. S., Todd, B. D., & Daivis, P. J. (2011). Prediction of fluid velocity slip at solid surfaces. *Phys. Rev. E 84, 016313* .

Hartkamp, R., Ghosh, A., Weinhart, T., & Luding, S. (2012). A study of anisotropy of stress in a fluid confined in a nanochannel. *J. Chem. Phys. 137, 044711* .

Joseph, S., & Aluru, N. R. (2008). Why are carbon nanotubes fast transporters of water? *Nano Lett. 8 (2)* , 452–458.

Li, T.-D., Gao, J., Szoszkiewicz, R., Landman, U., & Riedo, E. (2007). Structured and viscous water in subnanometer gaps. *Phys. Rev. B 75 115415* .

Lorenz, E., & Hoekstra, A. G. (2011). Heterogeneous multiscale simulation of suspension flow. *Multiscale Model. Simul. Vol 9, No. 4,* , 1301-1326.

Mackay, F. E., & Denniston, C. (2013). Coupling MD particles to a lattice-Boltzmann fluid through the use of conservative forces . *J. of Computational Physics 237* , 289–298.

Oden, J. T., Prudhomme, S., Romkes, A., & Bauman, P. T. (2006). Multiscale modeling of physical phenomena: adaptive control of models. *SIAM J. Sci. Comput. 28, No 6* , 2359-2389.

Popov, I. Yu. (2011). Statistical derivation of modified hydrodynamic equations for nanotube flows. *Phys. Scr. 83 045601* .

Prabha, S. K., & Sathian, S. P. (2012). Molecular-dynamics study of Poiseuille flow in a nanochannel and calculation of energy and momentum accommodation coefficients. *Phys. Rev. E 85, 041201* .

Reese, J. M., Zheng, Y., & Lockerby, D. A. (2007). Computing the Near-Wall Region in Gas Micro- and Nanofluidics: Critical Knudsen Layer Phenomen. *Journal of Computational and Theoretical Nanoscience, Volume 4, Number 4* , 807-813.

Shokouhmand., H., Meghdadi Isfahani, A. H., & Shirani, E. (2010). Friction and heat transfer coefficietns in macro and nano channels filled with porous media for wide range of Knudsen number. *Int. Comm. Heat Mass 37* , 890-894.

To, Q. D., Pham, T. T., Brites, V., Léonard, C., & Lauriat, G. (2013). Multiscale Study of Gas Slip Flows in Nanochannels. *Proc. ASME 2013 4th International Conference on Micro/Nanoscale Heat and Mass Transfer*, (p. V001T10A004).

Yang, S., Yu, S., Ryu, J., Cho, J.-M., Kyoung, W., Han, D.-S., et al. (2013). Nonlinear multiscale modeling approach to characterize elastoplastic behavior of CNT/polymer nanocomposites considering the interphase and interfacial imperfection. *Int. J. Plasticity 41* , 124-146.